Journal of The Electrochemical Society, **161** (1) A142-A148 (2014)
0013-4651/2014/161(1)/A142/7/$31.00 © The Electrochemical Society

Electrochemical Properties of Polyaniline-Coated Li-Rich Nickel Manganese Oxide and Role of Polyaniline Coating Layer

Dae-hyun Cho,[a] Hitoshi Yashiro,[b,*] Yang-Kook Sun,[c,d,*] and Seung-Taek Myung[a,*,z]

[a]*Department of Nano Science and Technology, Sejong University, Gwangjin-gu, Seoul 143-747, South Korea*
[b]*Department of Chemical Engineering, Iwate University, Ueda, Morioka, Iwate 020-8551, Japan*
[c]*Department of Energy Engineering, Hanyang University, Seoul 133-791, South Korea*
[d]*Department of Chemistry, King Abdulaziz University, Jeddah 21589, Saudi Arabia*

Polyaniline is coated on $Li[Li_{0.2}Ni_{0.2}Mn_{0.6}]O_2$ synthesized via co-precipitation. X-ray diffraction patterns exhibit that the polyaniline coating does not affect structural change of the $Li[Li_{0.2}Ni_{0.2}Mn_{0.6}]O_2$, and the resulting transmission electron microscopic images show the presence of coating layers on the surface of $Li[Li_{0.2}Ni_{0.2}Mn_{0.6}]O_2$. Electrochemical tests using coin type cells confirm that the surface modification by polyaniline is effective in maintaining capacity and retention upon cycling. The conducting coating character also assists improvement in rate capability. The polyaniline layer forms F-doped polyaniline during cycling, as is proved by time-of-flight secondary ion mass spectroscopy. Therefore, the presence of the polyaniline layers plays a role in lowering HF levels via scavenging F^- from HF in the electrolyte, and this F–doped polyaniline layer also assists in protecting the $Li[Li_{0.2}Ni_{0.2}Mn_{0.6}]O_2$ from HF attack upon cycling, resulting in improved electrochemical properties.
 [DOI: 10.1149/2.073401jes]

Manuscript submitted September 19, 2013; revised manuscript received October 18, 2013. Published November 26, 2013.

Owing to a large discharge capacity exceeding 200 mAh g^{-1}, over-lithiated manganese oxides ($Li[Li_xM_yMn_{1-x-y}]O_2$, M = Ni, Co) have been intensively studied for the last decade.[1–8] The structure allows lithium incorporation into transition metal layers such that the layer structure is stabilized though a large amount of Mn is introduced in the same layer. $Li(Co_{1-x}Li_{x/3}Mn_{2x/3})O_2$, which is comparable to $LiCoO_2$ in term of capacity, could be synthesized over the whole compositional range of $LiCoO_2$–Li_2MnO_3.[1,3,4] Substituting Co to Ni, $Li[Ni_{0.33}Li_{0.22}Mn_{0.55}]O_2$ delivers an exceptionally high capacity of 230 mAh g^{-1} in operation range between 2.0 and 4.6 V. Below 4.45 V, a reversible redox reaction of $Ni^{2+/4+}$ accompanies Li^+ deintercalation/intercalation though the resulting capacity is limited to 100 mAh g^{-1}, above which a long plateau results from simultaneous extraction of both Li and O from the crystal structure[6,7]

Efforts have been made to improve their intrinsic low rate capability stemming from the tetravalent Mn in the oxide matrix and cyclability as well. Hence, partial substitutions of Mn site with other elements or surface modifications have been made.[9–13] The addition of Co is obviously advantageous toward attaining a better rate capability although at the expense of capacity.[10,12] A recent report by Kang et al.[14] suggested that surface modification by $Al(OH)_3$ on $Li[Li_{0.2}Ni_{0.2}Mn_{0.6}]O_2$ was fairly effective in capacity retention, rate capability, and thermal stability. Similar effects were also reported using Al_2O_3 coating and $AlPO_4$ coating on the over-lithiated manganese oxides.[15,16] Those ceramic coating materials could decrease the charge transfer resistance during cycling, accomplishing better electrode performances. Although we do not know the reason that the attachment of a small amount of those coating materials contributed to the improved the electrochemical properties, improvement of cell performances is evident. We speculate that those coating materials would be a HF scavenger in the electrolyte, according to our previous studies.[17,18] Furthermore, we perceive the main problem of oxide coating to be difficulty in complete encapsulation of active materials like core-shell materials due to condensation and crystal growth of the coating materials even at mild heat-treatment condition; it, hence, shows an islands-like coating.[18] For the reason, we object to complete encapsulation of $Li[Li_{0.2}Ni_{0.2}Mn_{0.6}]O_2$ using a conductive polyaniline, which does not need further heat-treatment after polymerization. Also, the conductive coating layers are expected to improve the rate capability of the active material. In this paper, we introduce the details of polyaniline-coated $Li[Li_{0.2}Ni_{0.2}Mn_{0.6}]O_2$ and investigate the structural and the electrochemical properties and role of polyaniline layers on the surface of the active materials during cycling.

*Electrochemical Society Active Member.
zE-mail: smyung@sejong.ac.kr

Experimental

First, $(Ni_{0.25}Mn_{0.75})(OH)_2$ was prepared via the co-precipitation method. An aqueous solution of $Ni(II)SO_4 \cdot 6H_2O$ (Samchun) and $Mn(II)SO_4 \cdot 5H_2O$ (Junsei) (molar ratio of Ni:Mn = 1:3) with concentration of 2.0 mol L^{-1} was dropped into a reaction vessel stirring with 600 rpm under N_2 atmosphere. At the same time, NaOH solution (2.0 mol L^{-1}) and NH_4OH solution (1.2 mol L^{-1}) as a chelating agent were also separately added into the vessel by adjusting the solution pH to 12 at 50°C. Then the precipitated particles were filtered, washed, and dried in an oven at 80°C for 24 h. The obtained $(Ni_{0.25}Mn_{0.75})(OH)_2$ was heated to produce dehydrated $(Ni_{0.25}Mn_{0.75})_3O_4$ at 500°C for 5 h. The dehydrates were thoroughly mixed with an appropriate amount of LiOH (samchun) and calcined at 900°C for 15 h in air.

In attempt to modify the as-synthesized active materials with polyaniline (hereafter referred as to be PANi), Cl^--doped emeraldine salt state PANi ($[C_{24}H_{26}N_4(Cl)_2]_n$) was polymerized with aniline monomer ($C_6H_5NH_2$) and ammonium persulfate ($(NH_4)_2S_2O_8$,). First, aniline monomer and ammonium persulfate were separately poured into 1M HCl aqueous solution, and they were mixed to self-polymerize for 2 days. And the produced PANi in the solution was rinsed with absolute ethanol and acetone to remove the residual monomer, oligomer, and low molecular weight organic intermediates. To prepare violet pernigraniline base state (hereafter referred as to be VPB) PANi which needs to be dissolved in *N*-methyl-2-pyrrolinon(NMP) or *m*-cresol and so on,[19,20] the Cl^-– doped PANi was poured into a 1M NaOH aqueous solution and continuously stirred at 350 rpm for 2 days. Then, the solution was dried at 80°C in air. The obtained VPB powders were mixed with campor-10-sulfonic acid, β (CSA, Sigma-aldrich, with a ratio of 4:1 in weight) to prepare $(SO)_3^{2-}$– doped emeraldine salt state (hereafter referred as to be ES) PANi and dissolved into *N*-methyl-2-pyrrolinon (NMP). The as-sythesized $Li[Li_{0.2}Ni_{0.2}Mn_{0.6}]O_2$ powders were added into the solution and vigorously stirred to finally coat the ES-PANi homogeneously at 60°C. The NMP in the solution was evaporated in this stage. The coated amounts of the ES-PANi were 1 wt% and 2 wt% for the as-synthesized $Li[Li_{0.2}Ni_{0.2}Mn_{0.6}]O_2$. This method facilitates the active material to be modified under milder condition compared to the previous report,[21] which coated the active material under severe condition under HCl. Finally, the ES-PANi-coated $Li[Li_{0.2}Ni_{0.2}Mn_{0.6}]O_2$ samples were produced as described in Scheme 1, which explains the detailed procedures for ES-PANi-coated $Li[Li_{0.2}Ni_{0.2}Mn_{0.6}]O_2$.

X-ray diffractometry (XRD, Rint-2000, Rigaku) and high-resolution transmission electron microscopy (HR-TEM, JEM-3010, JEOL) were employed to characterize the synthesized powders. Time-of-flight secondary ion mass spectroscopy (ToF-SIMS, PHI TRIFT V nanoTOF, ULVAC-PHI) was also used to confirm the presence of the

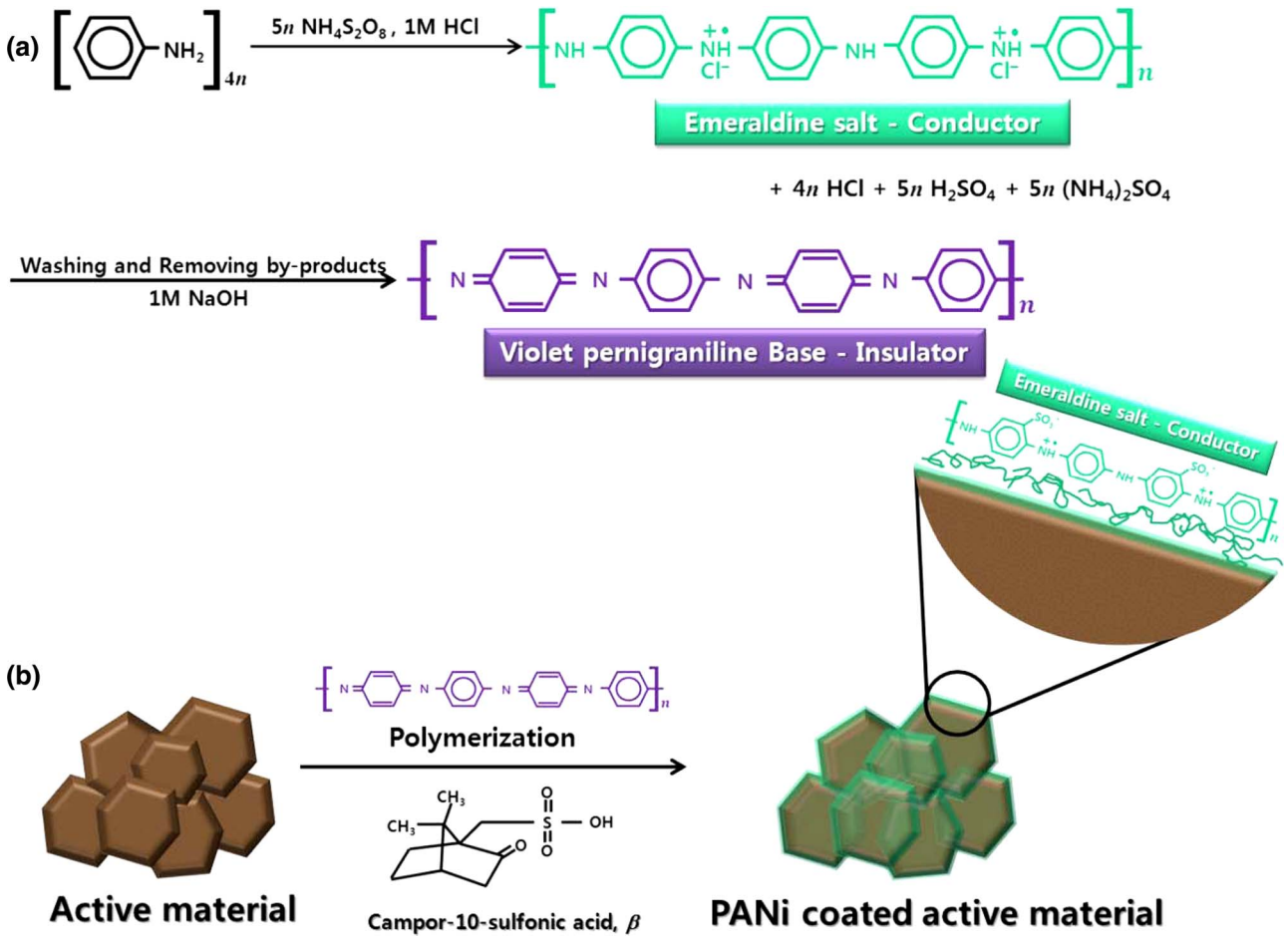

Scheme 1. ES-polyaniline coating procedures; (a) VPB-polymerization of polyaniline, (b) ES-polyaniline coating on surface of the active material.

ES-PANi layer on the surface of the $Li[Li_{0.2}Ni_{0.2}Mn_{0.6}]O_2$ powders. The chemical compositions of the final powders were determined by atomic absorption spectroscopy (AAS, Vario 6, AnalyticJena).

For the fabrication of positive electrodes, the as-synthesized and the surface modified $Li[Li_{0.2}Ni_{0.2}Mn_{0.6}]O_2$ powders were mixed with conductive materials (Super-P and Ketjen black, 1:1 in weight) and polyvinylidene fluoride in a weight ratio of 8:1:1 in NMP. The obtained slurries were applied onto Al foil and dried at 80°C in air. The electrodes were transferred to a vacuum oven and dried at 110°C overnight prior to use. Coin-type cells (2032) were assembled using Li metal (Honjo chemical) as a negative electrode in an argon-filled glove box. The electrolyte used was 1M $LiPF_6$ in ethyl carbonate–dimethyl carbonate (3:7 in volume, PanaX). The cells were charged and discharged between 2.0 and 4.7 V by applying various currents for electrochemical tests at room temperature. AC impedance measurements were performed in the frequency range of 1 MHz to 1 mHz with an amplitude of 10 mV.

For HF titration, the cycled cells were carefully disassembled and all contents were washed with salt-free solvent in the glove box for several days. NaOH aqueous solution and Bromothymol Blue as an indication solution were used for the titration of the cycled electrolyte.

To identify the presence of byproducts on the surface of the active materials after cycling, the cycled active materials were measured using a ToF-SIMS surface analyzer operated at 10^{-9} Torr, equipped with a liquid Ga ion source and pulse electron flooding. During the analysis, the targets were bombarded by the 10 keV Ga beams with a pulsed primary ion current varying from 0.3 to 0.5 PA. The total collection time was 100 s and rastered over a 120 μm × 120 μm dimension.

Results and Discussion

Figure 1 shows XRD patterns of bare and surface-modified $Li[Li_{0.2}Ni_{0.2}Mn_{0.6}]O_2$. The XRD patterns could be identified as an α-$NaFeO_2$ structure with $R\bar{3}m$ space group. Some reflections between 20° and 25° (2θ) were due to the superlattice ordering of Li and Mn

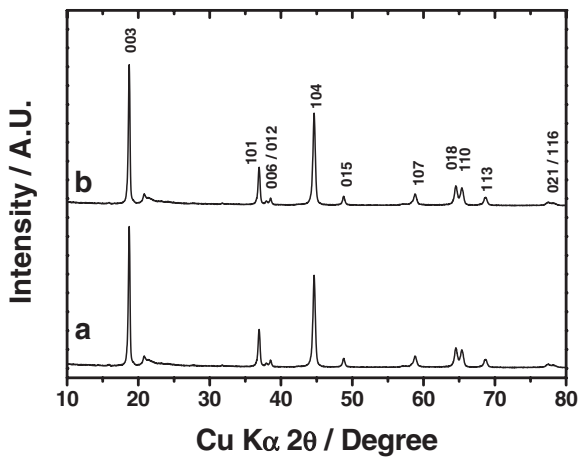

Figure 1. X-ray diffraction patterns of bare and polyaniline-coated $Li[Li_{0.2}Ni_{0.2}Mn_{0.6}]O_2$ powders: (a) bare and (b) 1 wt% ES-polyaniline-coated $Li[Li_{0.2}Ni_{0.2}Mn_{0.6}]O_2$.

Table I. Calculated lattice parameter of bare and 1 wt% ES-polyaniline-coated $Li[Li_{0.2}Ni_{0.2}Mn_{0.6}]O_2$.

	a-axis/Å	*c*-axis/Å
Bare	2.852(2)	14.224(2)
1 wt% ES-PANi-coated $Li[Li_{0.2}Ni_{0.2}Mn_{0.6}]O_2$	2.852(3)	14.224(4)

in the transition metal layers.[5] Though the $Li[Li_{0.2}Ni_{0.2}Mn_{0.6}]O_2$ was modified by a polymer layers, there are no significant difference in the XRD pattern compared to the bare- $Li[Li_{0.2}Ni_{0.2}Mn_{0.6}]O_2$. The calculated lattice parameters also indicated no change in the crystal structure before and after the surface modification (Table I). This is reasonable because the coating temperature was moderate as low as 60°C, such the condition is unlikely to affect structural change after the coating.

Since the coating medium is polymer, detection of the material was not possible using XRD. For this reason, the surface of the bare and the surface-modified $Li[Li_{0.2}Ni_{0.2}Mn_{0.6}]O_2$ were observed by TEM (Figure 2). The bare material showed clear edge lines, and no sediments were found on the surface (Fig. 2a). The coated materials had newly formed layers: 2–10 nm for the 1 wt% and 10–30 nm for the $Li[Li_{0.2}Ni_{0.2}Mn_{0.6}]O_2$ coated with 2 wt%. The coating layer was uniform for the 1 wt% coated sample but porous showing light contrast compared to the active material (Fig. 2b). Increasing the coating amount, however, it is obvious that the coating layers became aggregated (Fig. 2c).

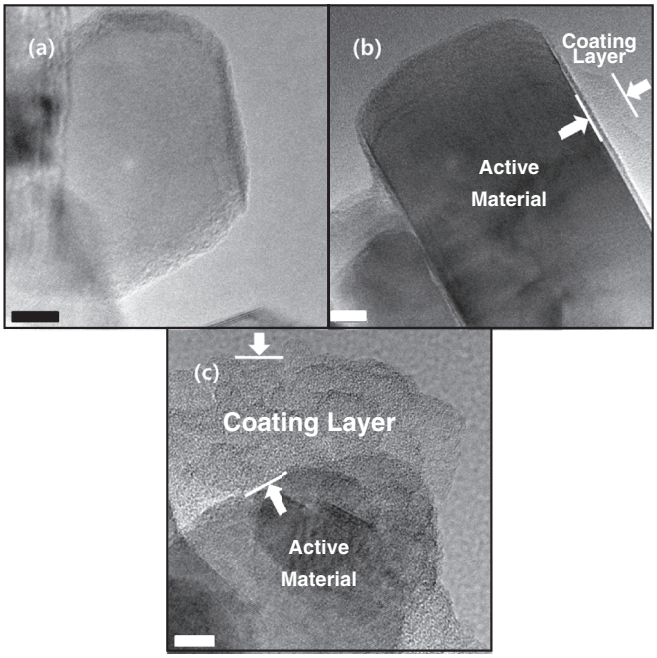

Figure 2. Bright-field TEM images of $Li[Li_{0.2}Ni_{0.2}Mn_{0.6}]O_2$; (a) bare, (b) 1 wt%, and (c) 2 wt% ES-polyaniline coated. The scale bar indicates 10 nm.

To clarify the coating layer on the surface of the $Li[Li_{0.2}Ni_{0.2}Mn_{0.6}]O_2$ material, the bare and the coated materials were analyzed by ToF-SIMS. Figure 3 shows a C_4HN^+(m = 63.01) fragment detected on the outermost surfaces of the active materials, which which is the clear evidence of the presence of ES-PANi coating layer on the $Li[Li_{0.2}Ni_{0.2}Mn_{0.6}]O_2$. Correlating the XRD, TEM, and ToF-SIMS data, the presence of ES-PANi coating layers did not induce structural change but the layers resided only on the surface of the active materials.

Figure 4 shows the first charge-discharge curves and the resulting differential capacities between 2.0 V and 4.7 V for the bare and the ES-PANi-coated $Li[Li_{0.2}Ni_{0.2}Mn_{0.6}]O_2$ measured at a constant current density of 20 mA g^{-1} at 25°C. For these electrodes, the electrochemical reaction occurred with two steps on charge (Figs. 4a and 4b): 2.0–4.5 V and 4.5–4.7 V.[22] In the first step, deintercalation of the lithium ion is obvious up to 4.5 V accompanying by the oxidation of Ni^{2+} to Ni^{4+}. In the second step, the long plateau above 4.5 V is related to the removal of Li_2O from the structure. The electrodes charged to 4.7 V exhibited three distinct sequences on discharge (Fig. 4b). The first two steps are found between 4.6 V and 3.9 V and between 3.9 V and 3.5 V due to the consequent reduction of Ni^{4+} to Ni^{3+} and Ni^{3+} to Ni^{2+}, respectively, after which Mn^{4+} is reduced to Mn^{3+} between 3.5 V and 2.9 V. From these results, we confirm that the coated electrode could reduce the first irreversible capacity, in particular, 1 wt% ES-PANi-coated electrode. Furthermore, the electrode delivered somehow higher capacity than that of the bare. Since the surface of $Li[Li_{0.2}Ni_{0.2}Mn_{0.6}]O_2$ is surrounded by the porous and uniform ES-PANi layers, the conducting coating layer is likely to assist improve capacity and, thereby, irreversibility as well. By contrast, the thicker and less homogeneous coating layers would be the reason for the slightly lower discharge capacity for the 2 wt% of ES-PANi-coated $Li[Li_{0.2}Ni_{0.2}Mn_{0.6}]O_2$ electrode, compared to that of the 1 wt% of ES-PANi-coated one.

The bare and the ES-PANi-coated $Li[Li_{0.2}Ni_{0.2}Mn_{0.6}]O_2$/Li cells were continuously cycled at a constant current density of 20 mA g^{-1}. The resulting charge–discharge curves and cyclability plots are shown in Figure 5. Although the first discharge capacity of the bare material showed a higher capacity than those of ES-PANi-coated electrodes, the capacity faded faster than the coated materials upon cycling. At the 50th cycle, capacity retentions of the cycled cells were approximately 78% for the bare, 88% for the 1 wt% of ES-PANi-coated and 91% for the 2 wt% of ES-PANi-coated electrodes. It is thought that the presence of ES-PANi coating layers would affect the discharge capacity and its retention upon cycling. The 1 wt% of ES-PANi coating seems to be better in terms of capacity and its retention, which is supported by the homogeneity of the coating layers shown in Fig. 2b. Hence, the experiments are further progressed for the bare and the 1 wt% of ES-PANi-coated $Li[Li_{0.2}Ni_{0.2}Mn_{0.6}]O_2$ to identify role of the ES-PANi coating layer attracting electrode performances.

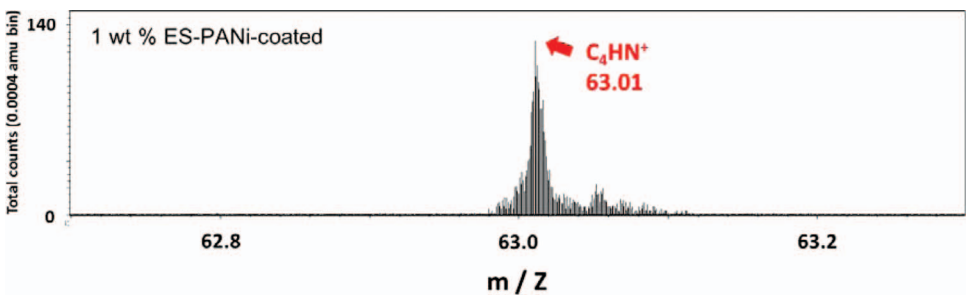

Figure 3. ToF-SIMS spectrum of 1 wt% ES-polyaniline coated $Li[Li_{0.2}Ni_{0.2}Mn_{0.6}]O_2$ powder.

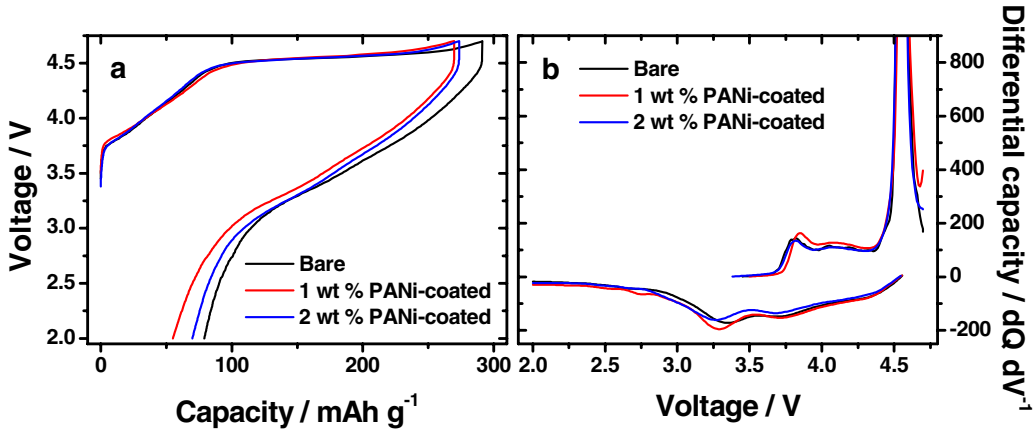

Figure 4. (a) The first charge/discharge curves and (b) differential capacities of the bare and ES-polyaniline coated $Li[Li_{0.2}Ni_{0.2}Mn_{0.6}]O_2$/Li cells at room temperature.

Figure 6 displays discharge curves of the bare and the 1 wt% of ES-PANi-coated $Li[Li_{0.2}Ni_{0.2}Mn_{0.6}]O_2$/Li cells at various currents ($1C$ = 210 mA g^{-1}) in the range of 2.0 V and 4.7 V. The cells were galvanostatically charged with a current of 20 mA g^{-1} prior to discharge. The discharge capacity of the bare material decreased faster with increasing *C*-rates relative to the coated material. It is suggested that the ES-PANi coating is effective in delivering capacity at high rates, probably due to its conductive character.

In order to understand the possible reasons for the improved electrochemical properties achieved by the ES-PANi coating on the $Li[Li_{0.2}Ni_{0.2}Mn_{0.6}]O_2$ particles, ac−impedance was employed to trace variation in the interfacial resistance between the electrodes and electrolyte (Fig. 7). It is clear that the ES-PANi-coated electrode exhibited a lower charge transfer resistance before and after the extensive cycling compared to the bare electrode. The presence of the conducting ES-PANi layer is likely to contribute to lowering the

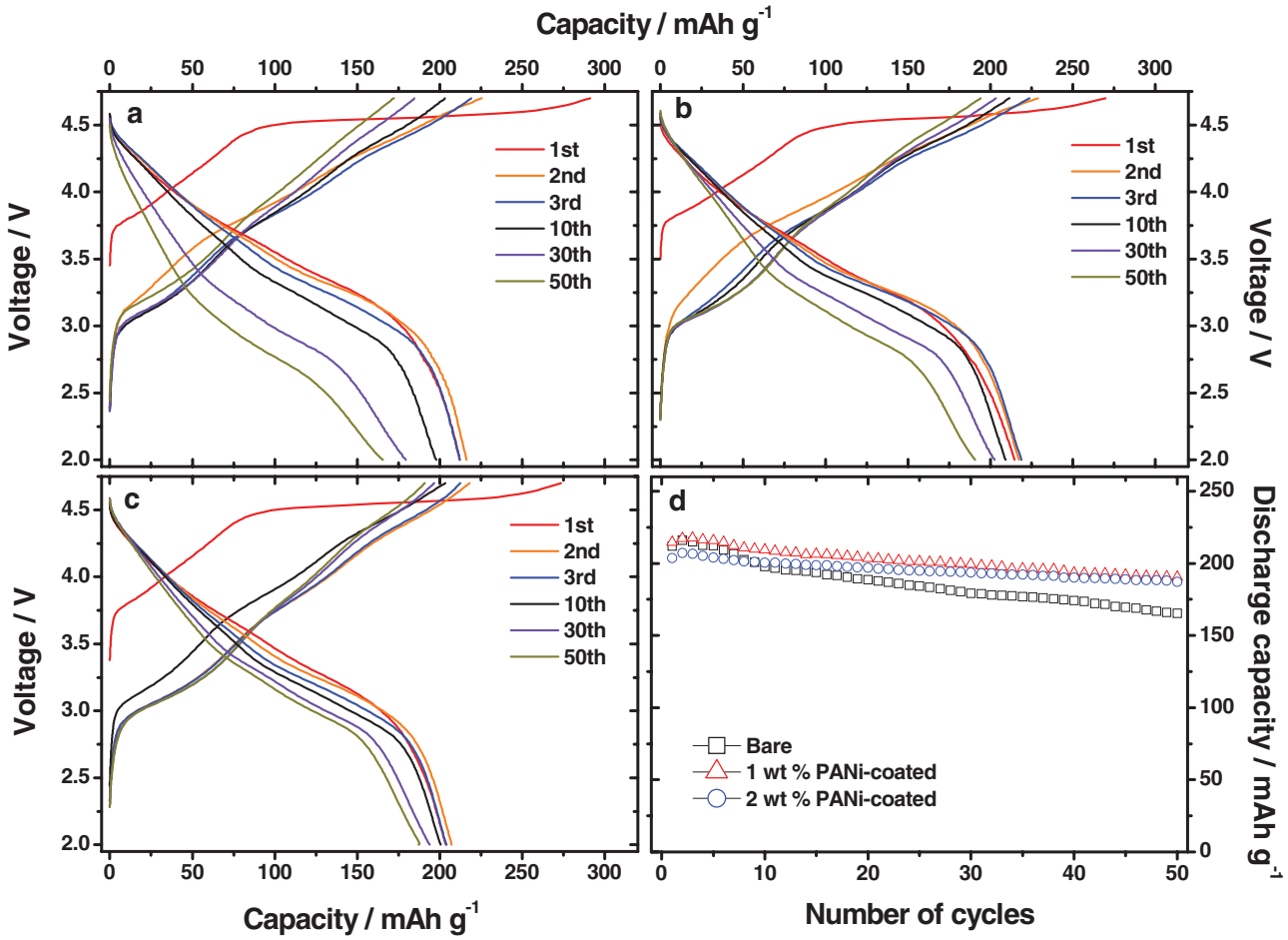

Figure 5. Charge and discharge curves of $Li[Li_{0.2}Ni_{0.2}Mn_{0.6}]O_2$/Li cells at room temperature; (a) bare, (b) 1 wt% ES-polyaniline-coated, (c) 2 wt% ES-polyaniline-coated, and (d) cyclability plots.

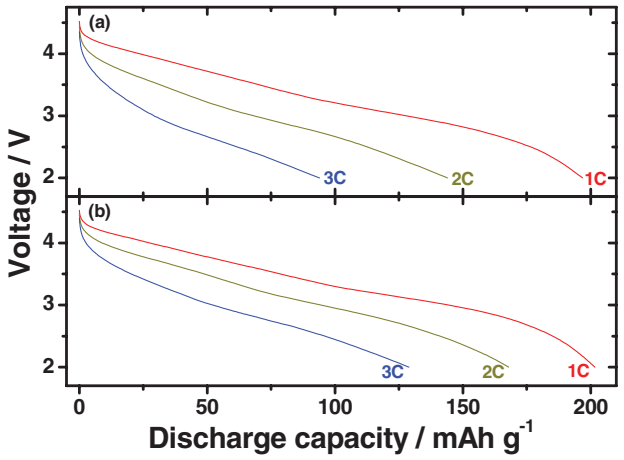

Figure 6. Rate capabilites of (a) bare and (b) 1 wt% ES-polyaniline-coated $Li[Li_{0.2}Ni_{0.2}Mn_{0.6}]O_2$/Li cells at room temperature. (1C = 300 mA g^{-1}).

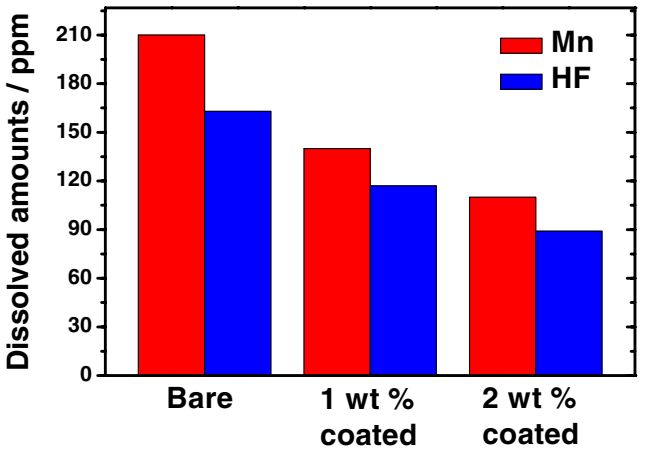

Figure 8. Acidic titration (as HF) and Mn dissolution results using cycled electrolytes for bare and ES-polyaniline-coated $Li[Li_{0.2}Ni_{0.2}Mn_{0.6}]O_2$/Li cells after extensive cycling at room temperature.

resistance, and this fact, in turn, results in the improved electrode performances.

To unveil the role of ES-PANi layer, the cycled cells were disassembled, and all components were rinsed with salt-free dimethyl carbonate for a week. HF titration was carried out using those solvents. In general, HF generation is common for alkyl carbonate electrolytes using $LiPF_6$ salt. This salt is unstable at elevated temperatures, high operation voltages and in the presence of water molecules. Since complete removal of water molecules, which appears as an impurity below 30 ppm for commercially available electrolytes, is impossible, formation of HF is inevitable as a result of the decomposition process of the electrolyte salt. Propagation is also facilitated at an elevated temperature and high operation voltage. As described in Fig. 8, the detected amount of HF was found to be 163 ppm for the bare electrode. Meanwhile, the amount of HF was reduced as low as 117 ppm for the 1 wt% ES-PANi-coated electrode and 82 ppm for the 2 wt% ES-PANi-coated one. It is notable that the voltage profile showed voltage drop caused by layer to spinel phase transformation for all samples (Fig. 4). This means that the structural change cannot be suppressed by the surface modification, as we previously reported in oxide coating system.[17,18] From the point of view, Mn dissolution from the active materials can be considered as one of the clues for the capacity fade. Thus, dissolved Mn ions in the cycled electrolyte were quantified by using AAS. As seen in Fig. 8, Mn ions were less dissolved for the ES-PANi-coated electrodes, and the content was

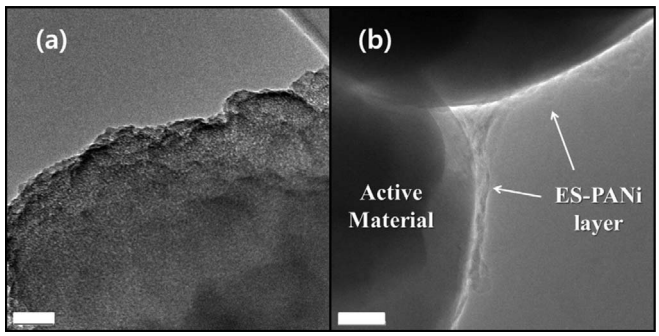

Figure 9. TEM images of cycled (a) bare and (b) 1 wt% ES-polyaniline-coated $Li[Li_{0.2}Ni_{0.2}Mn_{0.6}]O_2$ electrodes. The scale bar indicates 50 nm.

the lowest for the 2 wt% ES-PANi-coated electrode. Indeed, active materials were directly exposed to the electrolyte and continuously react with the propagated HF into the electrolyte. As a result, the surface of the bare material was severely damaged because of HF attack during electrochemical cycling (Fig. 9a). For the coated materials, the outermost surfaces were encapsulated by the PANi layers, so that the active materials would not have direct contact with the HF. The ES-PANi-coated material, thus, were able to keep the original smooth

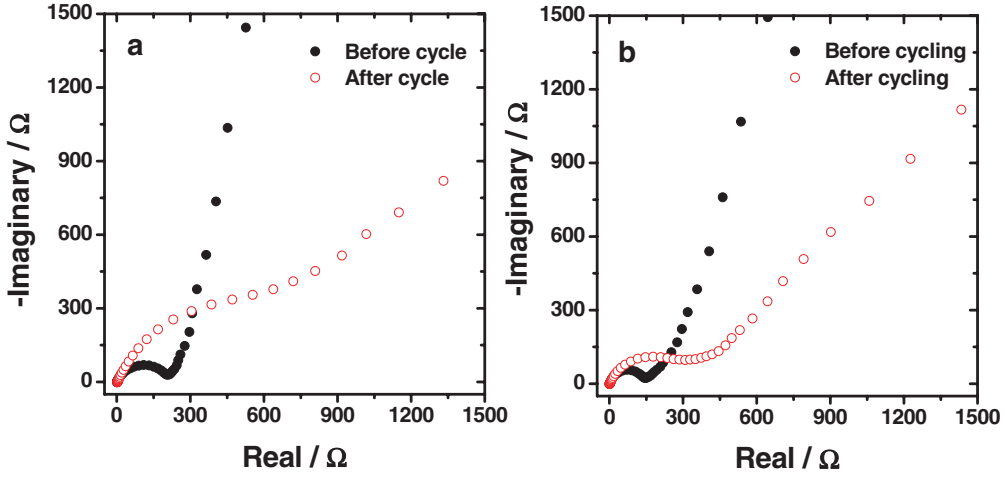

Figure 7. Ac-impedance spectra of (a) bare and (b) 1 wt% ES-polyaniline-coated $Li[Li_{0.2}Ni_{0.2}Mn_{0.6}]O_2$/Li cells before and after extensive cycling.

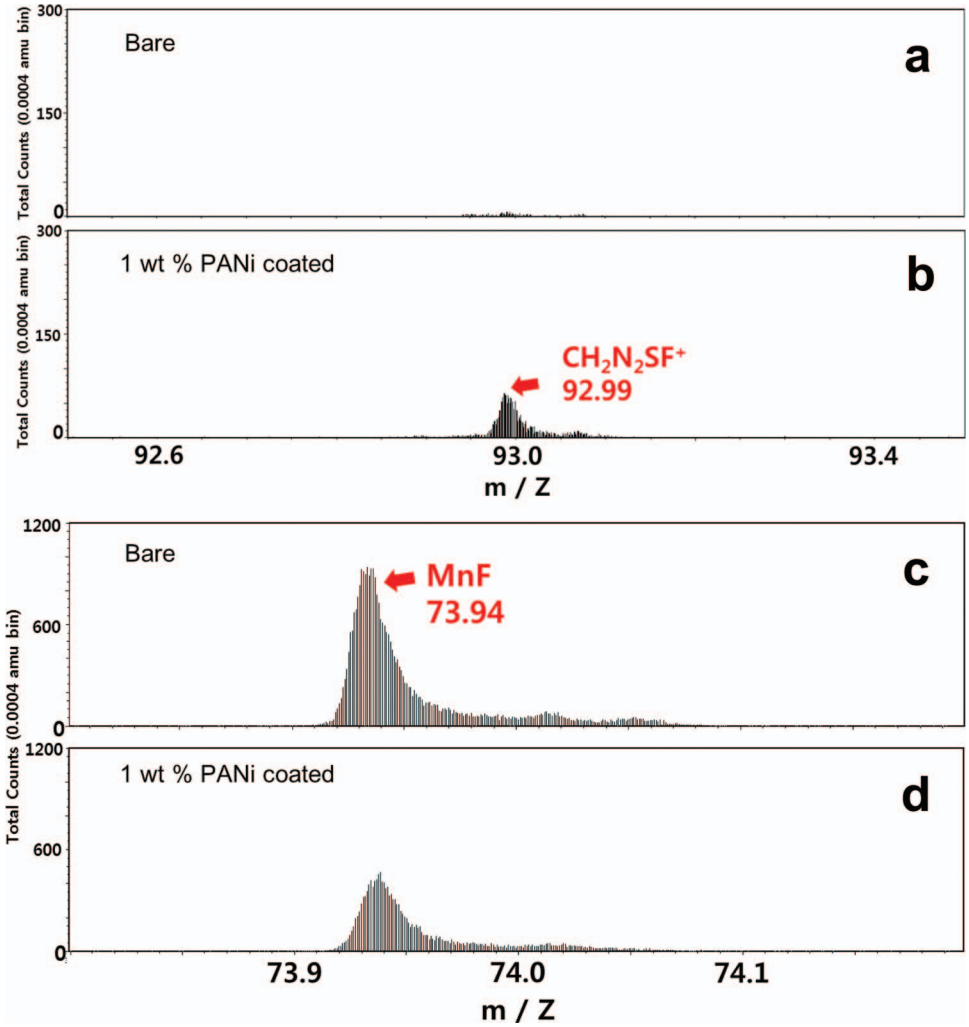

Figure 10. ToF-SIMS spectra of (a) $CH_2N_2SF^+$ fragment observed from the extensive cycled bare $Li[Li_{0.2}Ni_{0.2}Mn_{0.6}]O_2$ electrode, (b) $CH_2N_2SF^+$ fragment observed from the extensive cycled 1 wt% ES-polyaniline-coated $Li[Li_{0.2}Ni_{0.2}Mn_{0.6}]O_2$ electrode, (c) MnF^+ fragment from the cycled bare $Li[Li_{0.2}Ni_{0.2}Mn_{0.6}]O_2$ electrode, and (d) MnF^+ fragment from the cycled 1 wt% ES-polyaniline-coated $Li[Li_{0.2}Ni_{0.2}Mn_{0.6}]O_2$ electrode.

surface with the coating layer (Fig. 9b), because the ES-PANi could work as a shield against the HF attack. This reflects that less contact with the HF-propagated electrolyte induced less dissolution of Mn ions from the ES-PANi-coated active materials upon cycling. Summing, the ES-PANi-coated $Li[Li_{0.2}Ni_{0.2}Mn_{0.6}]O_2$ electrode exhibited better capacity, retention, rate capability, and lower impedance. In particular, the lower resistance seems to be highly related to the HF level in the electrolyte because the produced by-product, HF, readily decomposes active materials during cycling. The dissolved transition metals ions tend to be oxidized on the surface of positive electrode forming insulating oxides byproducts or reduced to metal causing metal plating on the surface of the negative electrode, which simultaneously increases cell impedance. Therefore, the reasons for the better electrode performance and lower impedance for the ES-PANi-coated $Li[Li_{0.2}Ni_{0.2}Mn_{0.6}]O_2$ electrodes are understood.

Although we found the reasons for the better electrode performances, the role of ES-PANi coating layers are not identified yet. The extensively cycled bare and ES-PANi-coated electrodes were analyzed by ToF−SIMS to explore how the coating layers react with electrolyte during cycling (Figs. 10a and 10b). The fragment observed at m = 92.99 is found to be $CH_2N_2SF^+$. The formation of HF is general when $LiPF_6$ salt was used as an electrolytic salt.[23,24] Similar to our prior reports such as Al_2O_3[17] and other metal oxides,[18] the ES-PANi layer would react with the produced HF during cycling:

$$[C_{24}H_{26}N_4(SO_3)_2]_n + 12HF \rightarrow [C_xH_yN_zS_\alpha F_\beta]_n + 6H_2O$$

The advent of the $CH_2N_2SF^+$ fragment indicates the presence of C−H−N−S−F chemical bonds (Fig. 10b), where the fragment was absent for the cycled bare (Fig. 10a), suggesting the gradual formation of F-doped ES-PANi coating layers by consuming the formed HF by-product in the electrolyte. Then, the HF level in the electrolyte could be reduced through the above reaction for the coated electrode so that the loaded active materials are less damaged during the prolonged cycling. Note, as a result, the lower intensity of MnF^+ fragment ES-PANi-coated electrode, which was ascribed to the Mn dissolution by followed reaction: $MnO + 2HF \rightarrow MnF_2$ (Figs. 10c and 10d). Hence, the propagation of lower amount of HF for the coated samples is understood. Furthermore, the ES-PANi coating layers would physically protect the surface of active materials from the HF attack as evident from the TEM image of Fig. 9b. Therefore, the surface modification using ES-PANi is effective in the improvement of capacity, retention, and rate capability. We conclude that the ES-PANi layer leads to lowering of the HF level in the electrolyte by scavenging HF, more likely F^-, in the electrolyte.

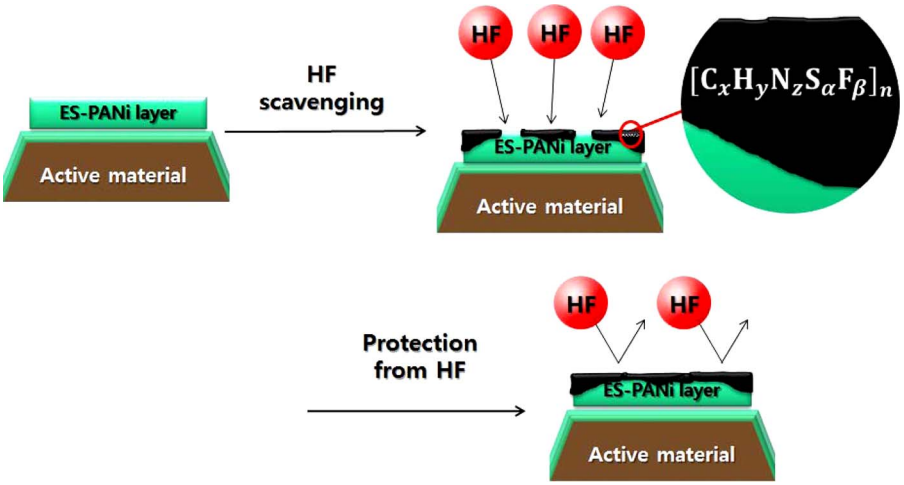

Scheme 2. Role of the ES-polyaniline coating layer on the surface of $Li[Li_{0.2}Ni_{0.2}Mn_{0.6}]O_2$ reacting with HF.

Conclusion

We investigate the effectiveness of ES-PANi coating for $Li[Li_{0.2}Ni_{0.2}Mn_{0.6}]O_2$ as a positive electrode material for lithium batteries. Although the surface modification did not affect structural changes and morphology shown in the results of XRD patterns and TEM images, the coating layer is formed uniformly because of the low temperature coating process, as designated. As a result, the ES-PANi-coated $Li[Li_{0.2}Ni_{0.2}Mn_{0.6}]O_2$ leads to improved capacity, retention, and rate capability with help of the conducting nature of the coating medium. ToF-SIMS analysis suggests that the ES-PANi coating layer forms, performing bifuncions such as scavenge HF and working as a protection layer from HF in the electrolyte (Scheme 2). Hence, ES-PANi-coated particles were kept upon extensive cycling. We suggest that present ES-PANi coating is applicable for not only $Li[Li_{0.2}Ni_{0.2}Mn_{0.6}]O_2$ but also any kinds of positive electrode materials.

Acknowledgments

The authors thank Miwa Watanabe, Iwate University, for her helpful assistance in the experimental work. This work was partially supported by the IT R&D program of MKE/KEIT [10041856, Technology development for life improvement of high Ni composition cathode at high temperature ($\geq$60°C)] and the secondary battery R&D program for leading green industry of MKE/KEIT [10041094, Development of Co-free, high thermal stability and eco-friendly layered cathode material for lithium ion batteries.]

References

1. K. Numata and S. Yamanaka, *Solid State Ionics*, **118**, 117 (2004).
2. Y. J. Park, Y.-S. Hong, X. Wu, M. G. Kim, K. S. Ryu, and S. H. Chang, *J. Electrochem. Soc.*, **151**, A720 (2004).
3. M. Balasubramanian, J. McBreen, I. J. Davidson, P. S. Whitfield, and I. Kargina, *J. Electrochem. Soc.*, **149**, A176 (2002).
4. B. Ammundsen, J. Paulsen, I. Davidson, R.-S. Liu, C.-H. Shen, J.-M. Chen, L.-Y. Yang, and J.-F. Lee, *J. Electrochem. Soc.*, **149**, A431 (2002).
5. Z. Lu, L. Y. Beaulieu, R. A. Donaberger, C. L. Thomas, and J. R. Dahn, *J. Electrochem. Soc.*, **149**, 78 (2002).
6. Z. Lu and J. R. Dahn, *J. Electrochem. Soc.*, **149**, A815 (2002).
7. S.-S. Shin, Y.-K. Sun, and K. Amine, *J. Power Sources*, **112**, 634 (2002).
8. Y.-S. Hong, Y. J. Park, X. Wu, K. S. Ryu, and S. H. Chang, *Electrochem. Solid State Lett.*, **6**, A166 (2003).
9. C. Pouillerie, L. Croguennec, Ph. Biensan, P. Willimann, and C. Delmas, *J. Electrochem. Soc.*, **147**, 2061 (2000).
10. D. Song, H. Ikuta, T. Uchida, and M. Wakihara, *Solid State Ionic*, **117**, 151 (1999).
11. V. Subramanian and G. T.-K. Fey, *Solid State Ionic*, **148**, 351 (2002).
12. S.-H. Kang and K. Amine, *J. Power Sources*, **119–121**, 150 (2003).
13. S. Levasseur, M. Menetrier, and C. Delmas, *J. Power Sources*, **112**, 419 (2002).
14. Y.-J. Kang, J.-H. Kim, S.-W. Lee, and Y.-K. Sun, *Electrochim. Acta*, **50**, 4784 (2005).
15. Y.-S. Jung, A. S. Cavanagh, Y. Yan, S. M. George, and A. Manthiram, *J. Electrochem. Soc.*, **158**, A1298 (2011).
16. Y. Wu, A. V. Murugan, and A. Manthiram, *J. Electrochem. Soc.*, **155**, A635 (2008).
17. S.-T. Myung, K. Izumi, S. Komaba, H. Yashiro, H.-J. Bang, Y.-K. Sun, and N. Kumagai, *J. Phys. Chem. C*, **111**, 4061 (2007).
18. S.-T. Myung, K. Izumi, S. Komaba, Y.-K. Sun, H. Yashiro, and N. Kumagai, *Chem. Mater.*, **17**, 3695 (2007).
19. J.-C. Chang and A. G. MacDiarmid, *Synth. Met.*, **13**, 193 (1986).
20. Y. Cao, P. Smith, and A. J. Heeger, *Synth. Met.*, **48**, 91 (1992).
21. Y.-M. Chung and K.-S. Ryu, *Bull. Korean Chem Soc.*, **30**, 8 (2009).
22. J.-S. Kim, C. S. Johnson, J. T. Vaughey, and M. M. Thackeray, *Chem. Mater.*, **16**, 1996 (2004).
23. D. Aurbach, *J. Electrochem. Soc.*, **136**, 906 (1989).
24. Edström T. Gustafsson and J. O. Thomas, *Electrochim Acta*, **50**, 379 (2004).